Structural Properties of Amorphous Bulk Fe, Co and Fe-Co Binary Alloys

R. Bellissent,[1] G. Galli,[2] T. Hyeon,[3] S. Magazu',[2]* D. Majolino,[2] P. Migliardo[2] and K. S. Suslick[3]

[1] Laboratoire Leon Brillouin, CEN Saclay, 91191 Gif sur Yvette Cedex, France
[2] Dipartimento di Fisica and I.N.F.M., Universita' di Messina, P.O. Box 55, 98166 S. Agata, Messina, Italy
[3] School of Chem. Sciences, University of Illinois at Urbana-Champaign, 505 S. Mathews Ave., Urbana, Illinois 61801, U.S.A.

Abstract

Elastic neutron diffraction experiments on amorphous iron, cobalt and their amorphous binary metallic alloys are presented. The measurements allow, for the first time, to describe the atomic distribution in samples obtained in the form of fine (<30 nm) amorphous elemental particles by sonochemical synthesis. In the case of a-Fe, the structural information from the shape of the radial distribution function is consistent with the Random Packing model (RPD) calculations previously made for films of amorphous iron. Finally the atomic magnetic moment of iron and cobalt in the amorphous bulk phase is also evaluated.

1. Introduction

Very recently amorphous *elemental* transition metals have been prepared by means of sonolysis of their metal organic compounds. As an example, the ultrasonic irradiation of solutions of volatile iron pentacarbonyl ($Fe(CO)_5$) yields a dull black powder [1, 2]. Acoustic cavitation occurs during ultrasonic irradiation of liquids, which forms localised hot spots that can have cooling rates as large as 10^9 to 10^{13} K/sec. This allows the preparation of non-crystalline solid metals, that previously were only prepared as thin films [3]. Whereas some elemental materials may be obtained in both crystalline and amorphous solid phases and in the liquid state, it has been very difficult to produce amorphous metals. There is extensive data (thoroughly reviewed by Chen [4]) on liquid metals, and also many theoretical proposals on non-crystalline solid metals. At present, however, very few experimental results are available on amorphous metals, mainly because of the great difficulties encountered in producing solid amorphous metals.

Among them, not only for its fundamental interest but also for practical applications, experimental data about the transition metals in the amorphous state and, particularly, on amorphous iron, cobalt and their alloys are of high interest in the field of material science. The current work presents new neutron diffraction results that can be considered as an extension to a-Co and to a-Fe-Co binary alloys of our previous study devoted to the analysis of the structure of amorphous iron [5].

2. Experimental procedure and data reduction

For these elastic neutron diffraction experiments, we used amorphous metal powders, sonochemically prepared, of pure Fe (a-Fe), pure Co (a-Co) and their alloys: Fe : Co = 5 : 1 (a-Co-Fe$_5$), Fe : Co = 1 : 1 (a-Co-Fe) and Fe : Co = 1 : 5 (a-Co$_5$-Fe) of molar ratio. The sample state

---

* Author for correspondence

was shown to be amorphous by X-ray and TEM micro-diffraction. Bulk elemental analysis determined the following weight percentage of impurities: (i) a-Fe (3.71%C, 0.60%H): (ii) a-Co (3.67%C, 0.36%H); (iii) a-Fe : Co = 5 : 1 (3.02%C, 0.43%H); (iv) a-Fe : Co = 1 : 1 (4.18%C, 0.70%H); (v) a-Fe : Co = 1 : 5 (4.29%C, 0.57%H). Neutron diffraction measurements were carried out on the 7C2 spectrometer on the hot source of the reactor Orphee of the Laboratory Leon Brillouin at Saclay. The samples were all weighted (samples sizes were between 500 mg and 1000 mg) and transferred under He atmosphere, from triple bottled containers filled under an Ar atmosphere into cylindrical, tight closed vanadium cells.

The use of a monochromatic neutron beam with a 0.7 Å wavelength provided us with a momentum transfer range from 0.3 to 16Å^{-1}, large enough to obtain accurate pair correlation functions $g(r)$ by Fourier transform. Measurements have been carried out at room temperature (~ 300 K) with a collecting time optimised for the different neutron scattering cross section of Fe and Co. For the latter, as an example, a typical run time of ~ 30 hours was required.

In Fig. 1 the neutron diffraction pattern $I(Q)$ vs. Q for pure a-Fe (a), a-Fe : Co = 5 : 1 (b), a-Fe : Co = 1 : 1 (c), a-Fe : Co = 1 : 5 (d) and pure a-Co (e) is presented. For comparison in Fig. 2 the diffraction intensity pattern of a previous our measurement on the pure a-Fe [5] is shown. As it can be seen from an inspection of Fig. 1, the amorphous nature of the samples is confirmed by the absence of sharp diffraction peaks, in agreement with the previous X-ray and electron micro diffraction data [1]. From the elemental analysis, a contribution was expected from the form factor of the residual hydrogen in a wide range of the explored Q. As previously discussed, the continuous line in Fig. 2 (curve 2-b) shows the shape of the hydrogen form factor that is present as residual in the sample. In addition, a residual magnetic moment is present in the amorphous iron that gives rise to a magnetic form factor [6] (curve 2-c).

Figure 3 shows the diffraction intensity pattern of pure a-Co (3-a). In the same figure the hydrogen form factor (3-b) and the magnetic form factor (3-c), are also represented. Both nuclear and magnetic intensities for Fe and Co have been normalised by comparison to the incoherently scattered intensity of a vanadium rod. As far as no magnetic correlation has been assumed, until now, the moment transfer dependence of the magnetic intensity is only coming from the Fe and Co form factors which are quite similar. Therefore, concerning the case of the alloys, magnetic intensity can be assumed to be a concentration weighed sum of Fe and Co contributions.
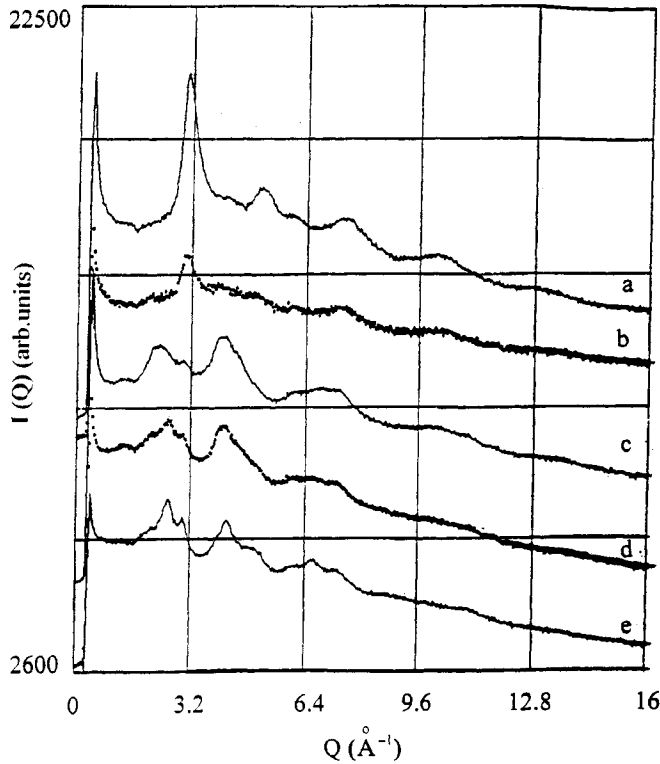
Fig. 1. Diffraction intensity pattern $I(Q)$ of pure a-Fe (a), a-Fe : Co = 5 : 1 (b), a-Fe : Co = 1 : 1 (c), a-Fe : Co = 1 : 5 (d) and pure a-Co (e). In order to clearly distinguish among them, a small shift in the vertical axis is applied.
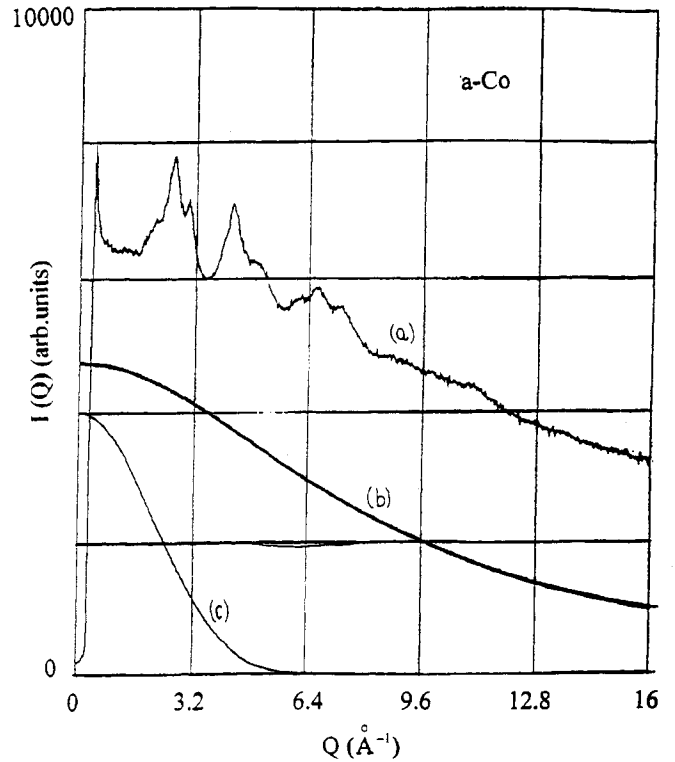

Fig. 3. Diffraction intensity pattern $I(Q)$ of a-Co. Points (a): experimental data, curves (b) and (c) refer to hydrogen and magnetic form factor. Notice that the curve (c) scale is magnified of factor 10.

3. Discussion

In order to obtain the static structure factor $S(Q)$ *vs.* Q, the intensity data were reduced following the classical method of Paalman and Pings [7] for the absorption correction by the container and the sample itself. The multiple scattering correction has been done following the Blech and Averbach [8] procedure. For each sample, the residual hydrogen contribution, has been removed. This consisted of a smoothly

Fig. 2. Diffraction intensity pattern $I(Q)$ of a-Fe. Points (a): experimental data, curves (b) and (c) refer to hydrogen and magnetic form factor. Notice that the curve (c) scale is magnified of a factor 10.

decreasing function of the momentum transfer, of the incoherent inelastic scattered intensity and was evaluated following a procedure due to Chieux *et al.* [9].

The static structure factors spectra were then Fourier transformed, and the pair correlation functions $g(r)$ obtained. As a matter of fact $g(r)$ has not been given in arbitrary units but normalised to 1 for large r, as the Fourier transform of the structure factor $S(Q)$:

$$g(r) = 1 + \frac{1}{2\pi^2 \rho r} \int_{-\infty}^{\infty} Q(S(Q) - 1) \sin (Qr) \, dQ \qquad (1)$$

Therefore the balanced cut-off oscillations at small r ensure a convenient choice of the bulk ρ. The found value is 0.065 at $Å^{-3}$ which is quite consistent with experimental determinations after sample elaboration.

In Figs. 4 and 5 the static structure factors $S(Q)$ *vs.* Q and the corresponding pair correlation functions $g(r)$ *vs.* r of pure a-Fe, pure a-Co, a-Fe : Co = 5 : 1, a-Fe : Co = 1 : 1, a-Fe-Co = 1 : 5 are plotted. It should be noticed that the structure factor exhibits a strong increase at very small momentum transfer. Such a feature, very common in amorphous systems can be related to long range density fluctuations (over 10 Å distances). It has been checked to have no effect on the Fourier transform for $r \geq 10$ Å. Such a behaviour could have been expected as far as the Fourier transform is the integral of $Q(S(Q) - 1)$ so that small Q range has no effect on the resulting $g(r)$. The low-Q side shoulder observed on the 1st peak of the structure factor is expected to be a real features because it is too sharp to be due to a wrong estimate of a hydrogen or magnetic corrections which both exhibit a very slow decrease in Q. In the case of a-Fe-Co binary alloys, it is to be noticed that the partial structure factor $S_{ij}(Q)$ can be evaluated by starting
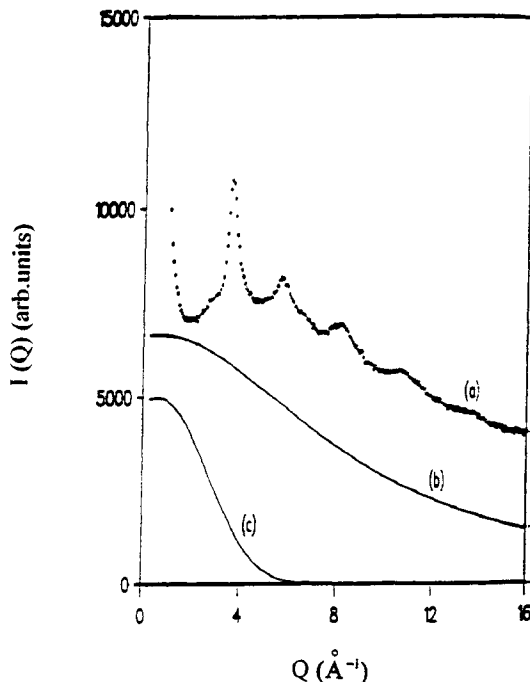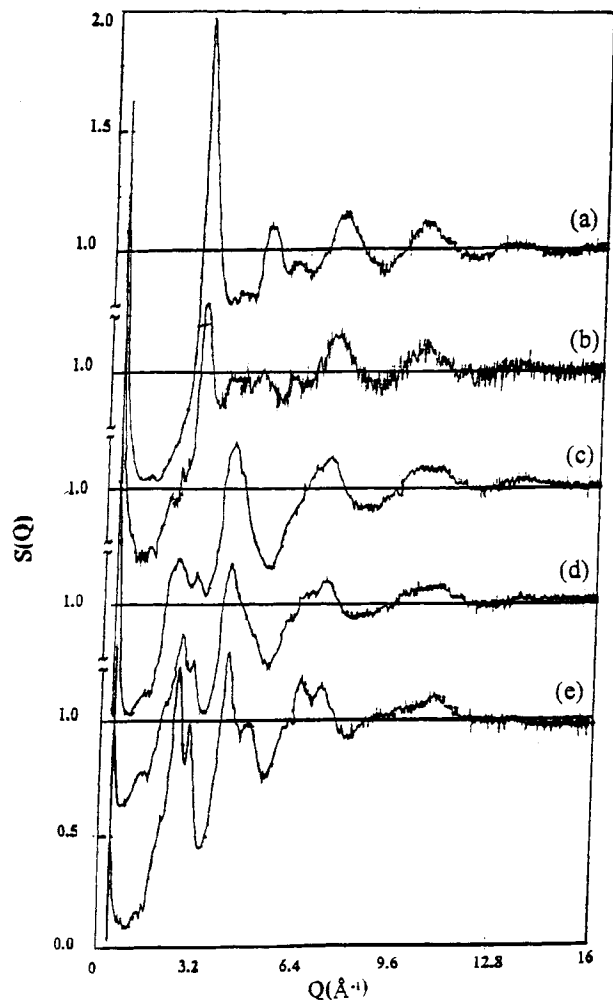
Fig. 4. Total static structure factor $S(Q)$ for: pure a-Fe (a); a-Co-Fe$_5$ (b); a-Co-Fe (c); a-Co$_5$-Fe (d) and pure a-Co (e).

Table I. *The weight factors of eq. (1) in the case of pure a-Fe, pure a-Co and of their binary mixtures*

	Fe-Fe $\dfrac{c_1^2 b_1^2}{\sum_i c_i b_i^2}$	Co-Co $\dfrac{c_2^2 b_2^2}{\sum_i c_i b_i^2}$	Fe-Co $\dfrac{2c_1 c_2 b_1 b_2}{\sum_i c_i b_i^2}$
a-Fe	1	0	0
a-Co-Fe$_5$	0.822	0.0022	0.087
a-Co-Fe	0.466	0.0314	0.248
a-Co$_5$-Fe	0.103	0.174	0.276
a-Co	0	1	0

from the following equation:

$$S(Q) = \frac{c_1^2 b_1^2}{\sum_i c_i^2 b_i^2} S_{11}(Q) + \frac{2c_1 c_2 b_1 b_2}{\sum_i c_i^2 b_i^2} S_{12}(Q)$$

$$+ \frac{c_2^2 b_2^2}{\sum_i c_i^2 b_i^2} S_{22}(Q) \qquad (2)$$

where b_i and c_i are the scattering length and the atomic fraction of the i-th component. The different coefficients, summarised in Table I, that enter in eq. (2) give rise to different weights of the contributions in partial structure factors. It turns out that, in the case of a-Fe : Co = 5 : 1 the Co-Co partial structure factor does not give a detectable contribution (0.22%) to the total structure factor evaluation, whereas the weight factor of Co-Co in the a-Fe : Co = 1 : case is several percent. The most relevant information that comes out from the analysis of the $g(r)$, i.e. the peak positions is summarised in Table II.
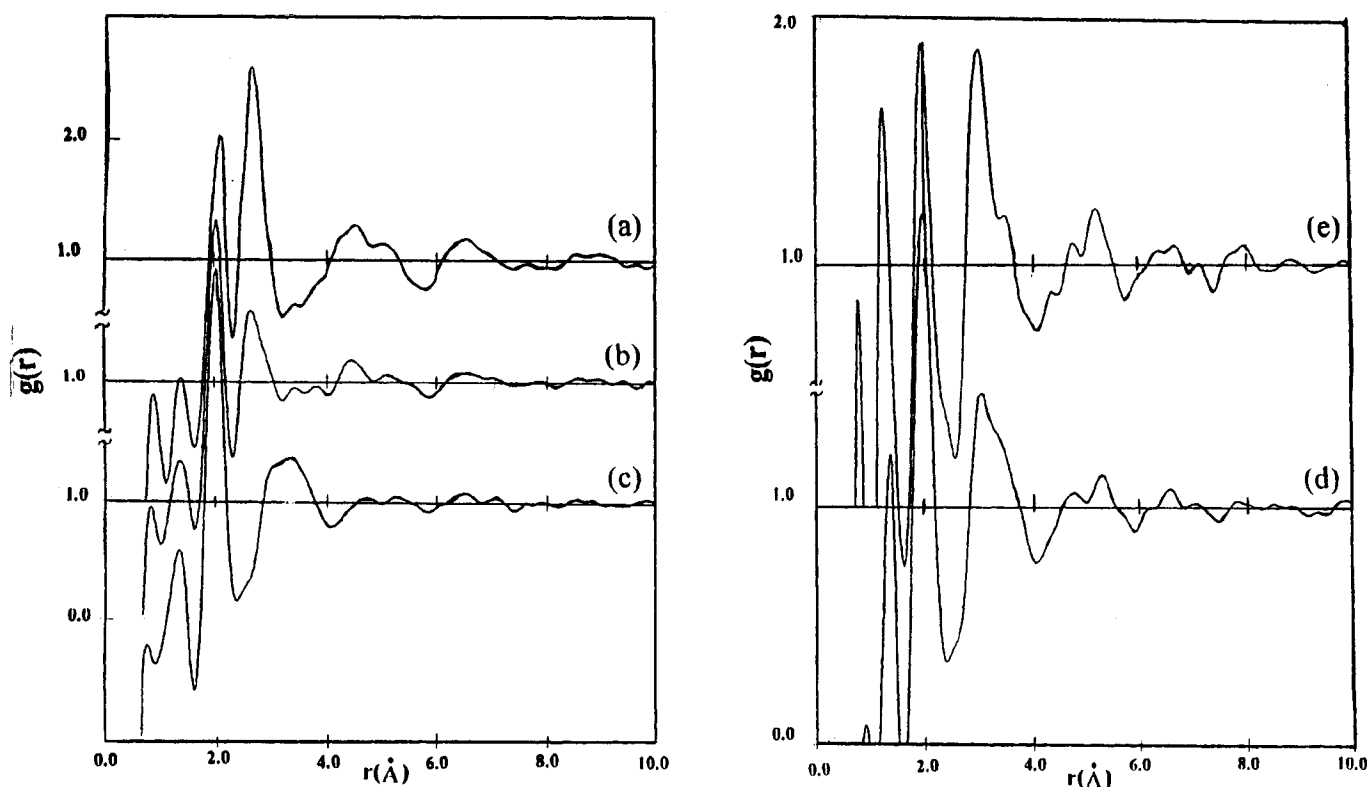

Fig. 5. Radial distribution function $g(r)$ for: pure a-Fe (a); a-Co-Fe$_5$ (b); a-Co-Fe (c); a-Co$_5$-Fe (d) and pure a-Co (e).

Table II. *Radial distribution function peaks maxima in pure a-Fe, in pure a-Co and in their binary mixture*

g(r), (Å)	0th peak	1st peak	2nd peak	3rd peak	4th peak
pure a-Fe			4.47	6.24	
	2.06	2.64		6.46	8.68
			5.02	6.51	
pure a-Co			4.75	6.34	
	1.97	3.05		6.46	7.74
			5.16	6.64	
a-Co-Fe$_5$			4.44	6.51	
	1.99	2.64		6.54	8.68
			5.08	6.98*	
a-Co-Fe		3.06	4.68	6.49	
	1.98			–	–
		3.38*	5.23*	7.04*	
a-Co$_5$-Fe		3.05	4.75	6.51	
	1.97			–	7.76
		3.36*	5.25*	6.98*	

Fig. 6. Q-dependence of partial static structure factors of liquid binary Fe-Co alloys: $\bigcirc$ $S_{Fe\text{-}Fe}(Q)$; $*$ $S_{Co\text{-}Co}(Q)$; $+$ $S_{Fe\text{-}Co}(Q)$.

As shown in Table II, the column designed 0th refers to a peak which is generally absent in previous neutron diffraction curves on binary metal-metalloid glasses. Its presence, in our sample, comes from the contribution of small amounts of Fe-O and Co-O bonds due to the residual oxygen. It is to be noticed, however, that the oxygen content of the sample is quite difficult to determine precisely without making assumptions on the exact way it is linked to the other components. The integration of the assumed metal-oxygen peak can be however an order of magnetic of about 20% atomic oxygen. For example, average Fe(III)-O distances [10] are 1.86 ± 0.06 Å, which is not inconsistent with our data analysis.

A discussion on the structure of amorphous iron and cobalt must be done in comparison with the results in crystals, liquid and glassy thin film. This last can be particularly useful because of the existence of previous diffraction data [11] and further structural analysis done by Ichikawa [12]. He noted a subpeak in the second peak of the radial distribution function, as we have in our RDF, that is present in many amorphous transition metals.

As in the case of pure a-Fe, also in the case of pure a-Co a dense random packing model (RDP) is suggested, in which the structure is, following the Ichikawa suggestions [12], built by "serially and densely piling up regular or slightly distorted tetrahedra around an assumed seed cluster".

In Table II, the peaks in the radial distribution function marked with stars could be referred to Fe-Co cross correlation maxima, because they are present only in the amorphous binary mixtures and not in the pure components. Their distances result infact quite different respect to that of pure a-Fe-Fe and pure a-Co-Co. In particular the higher distances of the first and second coordination shells of the cross-terms could indicate that the dense random-packing does not occur in these alloys and distorted tetrahedra or detect vacancies may be hypothesised to exist. This result, observed for the first time in these amorphous bulk binary alloys, is completely different than that observed in Fe-Co liquid binary alloys [13], as seen in Fig. 6, where the partial factor are shown.

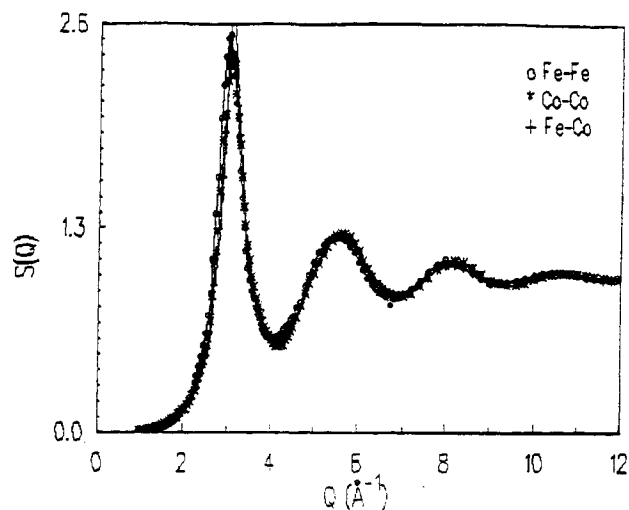Finally, some comments can be made about the atomic magnetic moment of these classes of amorphous solids.

The magnetic moments of amorphous iron and cobalt have been open problems in the physics of glassy metals, particularly in the relationship between topological disorder and magnetic properties of materials that, in normal conditions, would be ferromagnetic.

As we have previously discussed [5], the value of $\mu_{Fe} = 1.4 \mu_B$ has been obtained from direct experiments on amorphous iron. This agrees with the previously proposed parabolic dependence of magnetic moment *vs.* boron concentration in the binary iron-boron metallic glasses. Moreover it falls close to the value measured for the liquid, and it is reasonably consistent with the similarity between the features of the amorphous and liquid iron phases. In addition, the behaviour of the magnetic form factor in pure a-Co is very similar to that of iron.

4. Concluding remarks

Neutron diffraction data, obtained from samples of amorphous iron and cobalt powders prepared sonochemically, are, for the first time, presented. Diffraction data have been also obtained in their amorphous binary alloys. The structural information from the radial distribution function is consistent with a random packing model for the pure components, whereas a distorted tetrahedral structure is hypothesised to exist in the case of the binary mixtures. The analysis of neutron diffraction data will allow us to determine the magnetic moment μ contribution in the case of pure a-Fe and pure a-Co, that result very similar. A detailed analysis of the magnetic properties of pure a-Fe and of their mixtures with cobalt is actually under investigation by analyzing the polarized neutron elastic response.

References

1. Suslick, K. S., Choe, S. B., Cichowlas, A. A. and Grinstaff, M. W., Nature **353**, 414 (1991).
2. Grinstaff, M. W., Salamon, M. B. and Suslick, K. S., Phys. Rev. **B48**, 269 (1993).
3. Lauriat, J. P., J. Non-Crystall. Solids **55**, 77 (1983).
4. Chen, H. S., Rep. Prog. Phys. **43**, 353 (1980). See e.g. the comprehensive review of Y. Waseda: Y. Waseda "The Structure of Non-

Crystalline Materials: Liquids and Amorphous Solids" (McGraw-Hill Inc., N.Y. 1980) and reference therein.

5. Bellissent, R., Galli, G., Grinstaff, M. W., Migliardo, P. and Suslick, K. S., Phys. Rev. **B48**, 15797 (1993).
6. Petrillo, C. and Sacchetti, F., Solid State Comm. **74**, 543 (1990).
7. Paalman, H. H. and Pings, C. J., J. Appl. Phys. **33**, 2635 (1962).
8. Blech, I. A. and Averbach, B. L., Phys. Rev. **137A**, 1113 (1965).
9. Chieux, P., de Kouchkowski, R. and Boucher, B., J. Phys. **F14**, 2239 (1984).

10. International tables for X-ray Crystallography vol. III (Birmingham, Kynoch press) (1974).
11. Ichikawa, T., Phys. Stat. Sol. **A19**, 707 (1973).
12. Ichikawa, T., Phys. Stat. Sol. **A29**, 293 (1975).
13. The data of Fig. 6 are taken from the App. 9.7 of the Y. Waseda review book: Y. Waseda "The Structure of Non-Crystalline Materials: Liquids and Amorphous Solids" (McGraw-Hill Inc., N.Y. 1980) and reference theirein.